Planet. Space Sci. 1967, Vol. 15, pp. 817 to 824. Pergamon Press Ltd. Printed in Northern Ireland

A STATISTICAL ANALYSIS OF THE MARTIAN WAVE OF DARKENING AND RELATED PHENOMENA

JAMES B. POLLACK
Smithsonian Astrophysical Observatory and Harvard College Observatory

and

EDWARD H. GREENBERG
Smithsonian Astrophysical Observatory

and

CARL SAGAN
Harvard University and Smithsonian Astrophysical Observatory

(*Received* 7 *November* 1966)

Abstract—The progressive springtime darkening of the dark areas of Mars is discussed in terms of two models—one in which the darkening is due to biological activity in response to the increased temperature and humidity, the other in which fine dust is windblown off dark Martian highlands in spring. The observational data on darkening are subjected to a statistical-significance analysis. Although there are dark areas that are exceptions, a very significant correlation emerges between latitude and time of maximum darkening. Other significant correlations are found between brightness of a given dark area and time, between minimum and maximum contrasts of the dark areas during the seasonal changes, and between mimimum contrast and adjacency to bright areas—correlations expected on the dust models. The present data do not permit a choice between the biological and the windblown-dust models.

During local spring and summer, dark areas in a given hemisphere of Mars, as well as nearby equatorial dark areas in the opposite hemisphere, exhibit a marked darkening. Certain explanations (Focas, 1961, 1962) of this phenomenon have assigned an important role to water vapour, which is released into the atmosphere by the vaporization of the polar cap in the springtime hemisphere. In the most common development of this view, the darkening is attributed to the response of vegetation in the dark areas to the increased availability of atmospheric water vapour. Other hypotheses implicitly or explicitly invoke the seasonal transport of dust off and onto the dark areas (Sharonov, 1958; Kuiper, 1957; Rea, 1964; Sagan and Pollack, 1966a, 1967). In this paper we will carry out a statistical analysis of appropriate pairs of variables that describe the seasonal darkening to test these two models.

For many years observers of Mars have reported a correlation between latitude and the time of seasonal darkening. Darkening seems to occur earliest for areas of highest latitude and progressively later the more distant an area is from the springtime pole. This "wave of darkening" phenomenon clearly lends support to the water-vapour explanation of the seasonal darkening. However, the actual evidence favouring the existence of a *wave* of darkening is not immediately compelling.

Focas (1961, 1962) has carried out the only systematic photometric study of the seasonal darkening. Figure 1 displays a summary of his work, in which the degree of darkening at a given latitude, Λ, is indicated by the darkness of the crosshatching. The abscissa, η, the heliocentric longitude of Mars, varies progressively over the Martian year. Superposed on this diagram are isotherms computed from the inclination of the axis of Mars to its orbital plane and from the eccentricity of its orbit. The temperatures have been calculated for a transparent atmosphere and for a perfectly insulating surface with a bolometric albedo of 0·10. The temperatures indicated are mean temperatures from sunrise to sunset. Since the temperatures are determined only by the insolation, other choices of albedo will only change the labels on the isotherms. It would seem possible to fit any stage of the

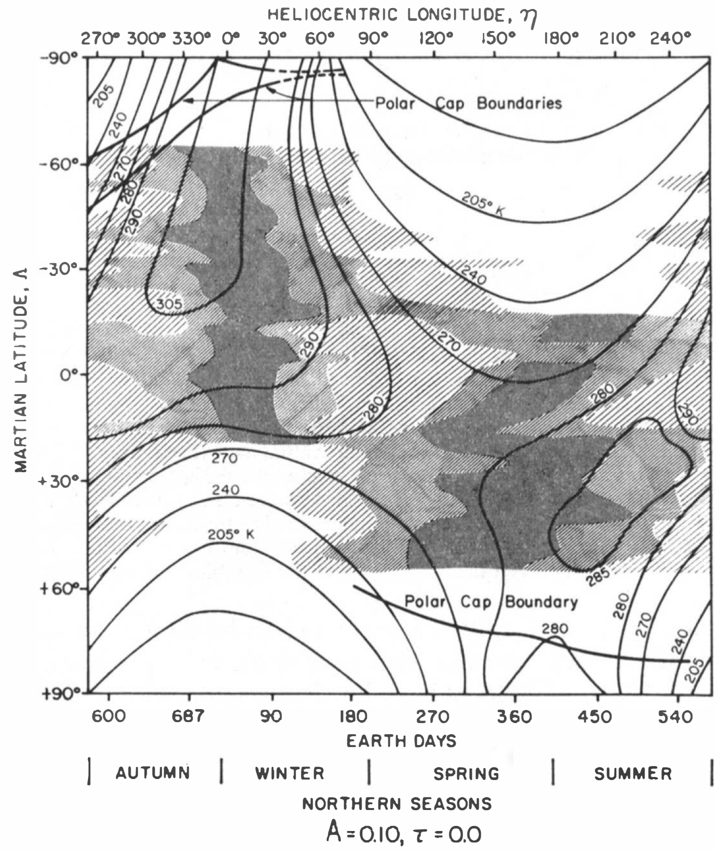

FIG. 1. DARKENING PHENOMENA ON MARS WITH ASSOCIATED SURFACE TEMPERATURES, ASSUMING ZERO THERMAL CONDUCTIVITY.
The shades of crosshatching correspond to maximum, intermediate, and minimum relative contrasts of dark and bright areas during the seasonal darkening.

darkening with a vertical line in Fig. 1, apparently implying the nonexistence of a *wave* of darkening. To investigate this matter more carefully we have subjected the best of Focas' data to a statistical analysis.

We have also attempted to find variables other than latitude to correlate with the time of darkening. Alternative variables are suggested by the dust model of the seasonal darkening, first advanced by Sharonov (1958), developed somewhat by Rea (1964), and recently converted into a model capable of quantitative predictions (Sagan and Pollack, 1966a, 1967).

Winds on Mars can be expected to exhibit a variation with both season and elevation. Around summer solstice, the temperature gradient between the equator and summer pole will be small and the winds in that hemisphere relatively mild. As a result, dust will rarely be lifted off the bright areas supposed here to be lowlands in agreement with radar and other evidence (Sagan and Pollack, 1966b; Sagan, Pollack, and Goldstein, 1966). Because of the tendency of winds to be stronger in highlands, however, dust will still be carried off the dark areas. In winter the winds are stronger generally and dust can be raised off both dark and bright areas. Smaller particles have higher albedos. Thus, around summer solstice there is a distinct net transport of fine particulate matter off dark areas and a consequent darkening of dark areas, while toward autumn there is a more balanced flow of material, with the dark areas possessing at any time some of the dust blown up from the bright areas (Sagan and Pollack, 1966a, 1967). Figure 1 illustrates the connection between shallow temperature gradients and darkening.

Several regularities are suggested by this model. There should be a statistical tendency for maximum darkening to occur at or after summer solstice—the net transport of dust off the dark areas will continue until the winds strengthen sufficiently. Those areas that are fairly isolated from and are situated high above surrounding bright areas should continue darkening longer. Thus, the dust model predicts a correlation of the brightness of dark areas with time of maximum darkening, in the sense that darker areas achieve maximum darkening later. A weaker correlation is expected between the proximity of a dark area to a bright area and the time of darkening, since the elevation of the dark area also plays a role in determining its darkness.

So far we have considered only time correlations. Two other correlations are suggested by the dust model. The brightness of an area during darkening should be closely connected with the brightness before and after darkening. The ranking of areas according to brightness should be quite similar in all three cases. (We note, however, that biological darkening models may make similar predictions.) Also, a moderate correlation should exist between brightness and adjacency to bright areas, with the brighter dark areas being systematically closer to the desert areas.

We will now discuss the sources of the variables discussed above and then outline the correlation procedure.

Focas has performed a large number of photometric measurements of photographs of Mars to determine the change of brightness of various dark areas over a complete run of seasons (360° of heliocentric longitude). The brightness of a given dark (Fr., sombre) area, B_s, was corrected for limb-darkening and phase-angle effects and compared with the brightness, B_c, of bright (Fr., claire) areas located at the centre of the disc; i.e. the ratio B_s/B_c was determined. For each dark area, Focas plotted the individual determinations of B_s/B_c against heliocentric longitude and drew a mean curve through them. At a given opposition, Mars is close enough to the Earth to permit photographs of acceptable resolution for only a limited range of heliocentric longitudes. This circumstance forced Focas to combine the observations of eight oppositions in order to obtain a complete run of η; i.e., he combined seasons from different Martian years. However, the data points from different oppositions seem to fit fairly smoothly on the mean curves. For our purposes we will be concerned with observations that span several oppositions. One opposition is that of 1956, during which a planetary-wide dust storm occurred, which might cause significant irregularities in the darkening pattern. The dust storm began at high latitudes and then spread toward the equator.

For each dark area measured by Focas we have attempted to determine the time of the beginning, end and maximum of the darkening progression. In each case we require a sufficient number of data points to determine accurately each of these times. With this condition fulfilled it is rather easy to locate the heliocentric longitude of maximum darkening for a given area. It is much more difficult to locate the longitudes of commencement and termination of the darkening, because of errors of measurement and intrinsic variations of the brightness outside the times of extensive darkening. We can see, for example, that a dark area undergoing minimal darkening might appear to begin later and end earlier than one with a larger degree of darkening. As a result, little confidence can be placed in measurements of the beginning and ending of darkening, but the time of maximum darkening can be well established in many cases. For several areas our estimates of the times of maximum darkening, based on Focas' graphs, differ from the times he mentions in his text. Focas' graphs are the primary source of information. However, to check the graphs and assure ourselves of the absence of systematic displacements or distortions, we have examined the overlapping left- and right-hand ends of the contradicted curves. Points at the two ends should be located at the same heliocentric longitudes if the curves are undistorted. This proves to be the case.

The average distance, L, from the centre of a dark area to adjacent, prominent bright areas was measured on the map of Mars prepared by Dr. A. Dollfus and distributed by the Space and Information Systems Division, North American Aviation, Downey, California. It is quite similar to the International Astronomical Union Mars cartography. The parameter L was found by measuring the distance l_i to a bright area in the east, west, south and north directions and calculating the harmonic mean of these quantities:

$$\frac{1}{L} = \frac{1}{4}\sum_{i=1}^{4}\frac{1}{l_i}. \tag{1}$$

Note that the value of L for an area surrounded by bright areas on two sides is twice the value that would obtain if the area were completely surrounded by bright areas. On the other hand, an arithmetic mean of l_i would diverge. Thus, the harmonic mean is a more suitable averaging procedure within the context of the dust models—in the example above, the area surrounded on two sides would certainly experience some interchange of dust with its neighbouring bright areas. While some subjectivity enters in our deciding whether an adjacent area is a prominent bright area, and so affects the measurement of l_i, it is still quite easy to distinguish between dark areas with centers close to bright areas, such as Tithonius Lacus, and those with larger displacements of centres, such as Mare Cimmerium. On this same map of Mars there is a listing of the location of the centres of the dark areas.

Table 1 summarizes the basic observational data. It lists the heliocentric longitudes, η, at the beginning, maximum, and end of darkening during southern summer. Season and time progress as the heliocentric longitude varies from 280° to 360° (equal to 0°) to 100°. Also specified are L, the latitude Λ, the time Δt between maximum darkening and summer solstice in terrestrial days, the average relative brightness $(B_s/B_c)_{\min}$ prior to and after darkening, and the relative brightness $(B_s/B_c)_{\max}$ at the height of darkening. When an equatorial area is alternately subject to darkening during summer in both hemispheres, an average value of $(B_s/B_c)_{\max}$ is used. A minus sign for Λ indicates the area is in the southern hemisphere and a plus sign for Δt signifies that maximum darkening was reached after summer solstice. There were not enough dark areas with well-defined brightness curves to permit a meaningful statistical analysis of the northern darkening phenomena, and so we will be concerned only with the southern data.

Table 1 suggests that there are obvious exceptions to the hypothesis of a wave of darkening. For example, Tithonius Lacus, which is almost at the equator, begins its darkening earlier than any other dark area and reaches its maximum darkening at a time similar to those for the highest latitude regions. One therefore must modify the wave-of-darkening concept to a statistical picture and postulate that local inhomogeneities, either among the dark areas themselves and/or in local atmospheric conditions, account for individual exceptions to the general rule. It might be noted that the dust model predicts the early maximum of darkening for Tithonius Lacus, because of its high value of (B_s/B_c) and its adjacency to bright areas. With the exception of Depressio Hellespontica, maximum darkening is always achieved after summer solstice. We now outline the statistical test applied to the data in Table 1.

TABLE 1. BASIC DATA

	Λ	η_{begin}	η_{max}	η_{end}	L (km)	$(B_s/B_c)_{\text{min}}$	$(B_s/B_c)_{\text{max}}$	Δt (days)
1. Depressio Hellespontica	−60°	—	345°	—	435	0·730	0·480	−25
2. Mare Chromium	−58	—	0	—	414	0·700	0·560	+ 4
3. Aonius Sinus	−45	—	0	50°	425	0·685	0·550	+ 4
4. Phrixi Regio	−40	—	25	—	660	0·700	0·570	52
5. Mare Hadriacum	−40	310°	10	80	320	0·675	0·500	23
6. Mare Sirenum	−30	—	5	—	747	0·630*	0·450	13
7. Mare Serpentis	−30	330	20	120	362	0·610	0·450	42
8. Solis Lacus	−28	350	15	95	517	0·650	0·450	32
9. Pandorae Fretum	−25	—	5	105	348	0·780	0·480	13
10. Mare Erythraeum	−25	320	15	60	1258	0·700	0·520	32
11. Mare Tyrrhenum	−20	350	32·5	85	1128	0·675	0·520	66
12. Mare Cimmerium	−20	290	30	90	1231	0·635	0·475	61
13. Iapigia	−20	320	5	—	1355	0·685	0·500	13
14. Aurorae Sinus	−15	340	22·5	80	763	0·630	0·500	47
15. Margaritifer Sinus	−10	340	20	80	645	0·650	0·480	42
16. Sinus Sabaeus	− 8	330	30	80	352	0·575	0·500	61
17. Sinus Meridiani	− 5	360	35	90	650	0·525	0·470	71
18. Tithonius Lacus	− 5	280	0	80	321	0·800	0·610	4
19. Syrtis Major	+10	320	10	90	865	0·570	0·440	23
20. Lunae Palus	+15	350	20	70	527	0·800	0·600	42

* Focas' value for B_s/B_c prior to darkening is listed as equal to the value at maximum darkening. This is clearly a misprint and so only the value of B_s/B_c after darkening was used here.

Suppose we wish to determine whether there is an association between two variables x and y, given a sample of N objects $\{(x_i, y_i)\}_{i=1}^{N}$. We compute the sample correlation coefficient r defined by the equation (Hoel, 1947)

$$r = \frac{\frac{1}{N}\left[\sum_{i=1}^{N} (x_i y_i - \bar{x}\bar{y})\right]}{\left[\frac{1}{N}\sum_{i=1}^{N} (x_i^2 - \bar{x}^2)\right]^{1/2}\left[\frac{1}{N}\sum_{i=1}^{N} (y_i^2 - \bar{y}^2)\right]^{1/2}}, \tag{2}$$

where $\bar{x}$ and $\bar{y}$ denote the average values of x and y. The correlation coefficient r has the following properties: (1) $|r| \leq 1$; (2) $r = \pm 1$ if there is a perfect linear correlation; and (3) $r = 0$ if there is no linear correlation. Negative values of r indicate that increasing values of x are associated with decreasing values of y.

Now consider the frequency distribution of r obtained from a large number of samples of fixed size N belonging to an infinite population $\{(x, y)\}$ with correlation coefficient ρ. To determine the significance of a particular value, r_0, obtained from a single sample of size N, we calculate the probability P_{r_0} that such a correlation should be exceeded by random sampling from an uncorrelated population. If P_{r_0} is low, we regard the correlation as significant.

For samples of small size the distribution of values of r is non-normal and for $\rho \neq 0$ it is asymmetrical, making the calculation of the probability exceedingly difficult. Fortunately, there exists a simple change of variables that transforms the complicated distribution of r into an approximately normal distribution. Applying Fisher's (1941) transformation

TABLE 2. CORRELATION BETWEEN PAIRS OF VARIABLES, DESCRIBING THE SEASONAL DARKENING

Variables correlated	Areas used	r Correlation coefficient	P Probability that the correlation is significant
η_{begin} and Λ	1–20	0·160	0·17
$\eta_{\max}$ and Λ	1–20	0·498	0·98
η_{end} and Λ	1–20	0·032	0·03
$\eta_{\max}$ and $(B_s/B_c)_{\min}$	1–18	−0·694	>0·99
$\eta_{\max}$ and $(B_s/B_c)_{\min}$	1–20	−0·509	0·98
$\eta_{\max}$ and L^{-1}	1–18	−0·386	0·88
$(B_s/B_c)_{\min}$ and $(B_s/B_c)_{\max}$	1–18	+0·557	0·99
$(B_s/B_c)_{\min}$ and L^{-1}	1–20	+0·296	0·79
$(B_s/B_c)_{\min}$ and Λ	1–20	−0·163	0·50

$$Z(r) = \tfrac{1}{2}\log_e \frac{1+r}{1-r} = r + \frac{r^3}{3} + \frac{r^5}{5} + \dots, \tag{3}$$

we obtain a new variable, Z, which is approximately normally distributed with variance $\sigma_Z = 1/\sqrt{(N-3)}$ and mean $\mu_Z = \tfrac{1}{2}\log_e[(1+\rho)/(1-\rho)]$ with the property that

$$P \equiv P(-r_0 \leq r \leq r_0) \simeq \int_{-Z(r_0)}^{Z(r_0)} f(z)\,dz = 1 - P_{r_0}, \tag{4}$$

where f is the density of the new distribution. It follows that P is the probability that the correlation is significant. For comparison with an uncorrelated population we set $\rho = 0$, i.e. $\mu_Z = 0$, and determine P from tables of normal density functions.

Table 2 summarizes the results of applying the statistical test outlined above to the data given in Table 1. It lists the pairs of variables correlated, the dark areas of Table 1 used, the correlation coefficient r and the probability P that the correlation is significant. The dust model makes an explicit time-correlation prediction only for dark areas located in the spring hemisphere. This meant a deletion of 2 areas from the sample 20 in carrying out the correlations of L and $(B_s/B_c)_{\min}$ with $\eta_{\max}$. However, as can be seen from Table 2, the inclusion of the two excluded regions for the $(B_s/B_c)_{\min}$, $\eta_{\max}$ correlation does not change P significantly.

There does not seem to be a significant correlation between latitude and the beginning or end of the darkening. But values of η for these terms are poorly known, and for this reason we did not attempt to correlate them with the other variables.

An excellent correlation of latitude with the well-determined values of $\eta_{\max}$ emerges. The times of maximum darkening occur when the polar cap has almost completely vaporized. Both of these results are consistent with water-vapour models of the seasonal darkening.

However, there is also an extremely strong correlation of $(B_s/B_c)_{\min}$ with $\eta_{\max}$, in agreement with the dust models. Other predictions of the dust model are also verified. There is a moderate correlation of $\eta_{\max}$ with L, the average distance to a bright area, which is not so strong as the first correlation. From the viewpoint of the dust model, the height of a dark area as well as its value of L determines the seasonal darkening it will experience. Accordingly, the correlation of $\eta_{\max}$ with L is not expected to be as great as with $(B_s/B_c)_{\min}$. This point is further illustrated by the moderate value of P found for $(B_s/B_c)_{\min}$ and L. Finally, a highly significant correlation between $(B_s/B_c)_{\min}$ and $(B_s/B_c)_{\max}$ is found: The lightest areas before the seasonal darkening tend to be the lightest during darkening. We have already pointed out that, with one exception, maximum darkening is achieved after summer solstice. This one exception may be attributed to local fluctuations in the wind pattern. It should be noted that in all cases the sign of the correlation coefficient is the predicted one.

The dust models are far from the point where an explicit prediction can be made as to latitude correlations with $\eta_{\max}$. However, part of the latitude correlation could conceivably result from a biased sample—i.e. regions of higher values of (B_s/B_c) tend to be located near the pole. Table 2 shows the correlation of $(B_s/B_c)_{\min}$ with Λ to be a rather weak one with the appropriate sign. The correlation, however, is a very unstable one. If the value of $(B_s/B_c)_{\min}$ for Lunae Palus is changed from 0·8 to 0·7, the correlation coefficient increases to slightly above 0·3 in absolute value.

It should be noted that if we were to accept the correlation between $(B_s/B_c)_{\min}$ and L as significant, we could not rule out the water-vapour models. For example, windblown dust could lighten the dark areas at the end of the darkening period without being responsible for the darkening itself. Similarly, the times of maximum darkening are correlated (cf. Fig. 1) not only with high temperatures and increased water vapour, consistent with biological models, but also with small latitudinal temperature gradients and low winds, consistent with dust models.

Depressio Hellespontica, at $\Lambda = -60°$, participates in the wave of darkening despite its almost polar latitude. However, the darkening maximum occurs at a time of high local insolation and high computed daytime surface temperature (cf. Fig. 1). Thus, the darkening of Depressio Hellespontica cannot be used to argue against biological models of the seasonal contrast changes, contrary to the conclusion of Rea (1964).

In conclusion, there are areas that distinctly violate the concept of an invariable wave of darkening, but there is a very significant correlation of latitude with time of maximum darkening. Both the biological and the dust models are consistent with the above statistical analysis of the seasonal-darkening phenomena, and a choice between these models must be made on other grounds.

Acknowledgement—We are grateful to Dr. J. H. Focas for a useful discussion. Mrs. Elinore Green assisted in the computations incorporated in Fig. 1. This research was supported in part by National Aeronautics and Space Administration Grant No. 09–015–023.

REFERENCES

FISHER, R. A. 1941. *Statistical Methods for Research Workers*, (8th ed.) Oliver and Boyd, Edinburgh.
FOCAS, J. H. 1961. *Ann. Astrophys.* **24**, 309.
FOCAS, J. H. 1962. *Planet. Space Sci.* **9**, 371.
HOEL, P. G. 1947. *Introduction to Mathematical Statistics.* John Wiley, New York; Chapman and Hall, London.
KUIPER, G. P. 1957. *Astrophys. J.* **125**, 307.
REA, D. G. 1964. *Nature, Lond.* **201**, 1014.

SAGAN, C. and POLLACK, J. B. 1966a. *Astro. J.* **71**, 178.
SAGAN, C. and POLLACK, J. B. 1966b. *Smithsonian Astrophys. Obs. Spec. Rep.* **224**, 45.
SAGAN, C. and POLLACK, J. B. 1967. In preparation.
SAGAN, C., POLLACK, J. B. and GOLDSTEIN, R. M. 1966. *Smithsonian Astrophys. Obs. Spec. Rep.* **221**; also *Astr. J.* In press.
SHARONOV, V. V. 1958. *Priroda Planet*, p. 507. Moscow.

Резюме—Прогрессивное потемнение темных областей Марса весной обсуждается на основании двух моделей—одной, в которой потемнение обусловлено биологической активностью, вызываемой наростанием температуры и влажности, другой, в которой мелкая пыль выветривается весной из горных местностей Марса. Обсервационные данные относительно потемнения подвергаются важному, с точки зрения статистики, анализу. Несмотря на то, что существуют темные районы, являющиеся исключением, выявляется весьма значительная корреляция между широтой и временем наибольшего потемнения. Другие важные корреляции обнаруживаются между яркостью определенного темного района и периодом времени между минимальным и максимальным контрастами темных районов во время сезонных изменений, а также между минимальным контрастом и близостью к ярко освещенным районам, иначе говоря корреляции, которые предвидятся на пылевых моделях. Существующая в данное время информация не расчитана на выбор между биологической и выветренной моделями.